The Journal of Engineering Geology, Vol.13, No.2, June, 2003.pp.171-191

심부 처분공동 주변 절리에서의 열수리역학적 거동변화

Thermohydromechanical Behavior Study on the Joints in the Vicinity of an Underground Disposal Cavern

김 진 웅(Jhinwung Kim)* 한국원자력연구소 방사성폐기물처분연구부
배 대 석(Dae-seok Bae) 한국원자력연구소 방사성폐기물처분연구부

요약 / ABSTRACT

본 연구의 목적은 고준위 방사성폐기물을 지하 심부 불연속 화강 암반 내에 처분할 때 처분공동 주변 절리에서의 장기간(500년)에 걸친 열수리역학적 연성거동 변화를 분석하고, 앞으로 처분 개념 설정에 활용 하고자 하는 것이다. 해석모델은 포화된 불연속 화강 암반, 처분공내 압축 벤토나이트로 둘러 쌓인 PWR 사용후 핵연료 및 처분용기, 그리고 처분동굴 내에 채워진 혼합 벤토나이트를 포함한다. 해석모델 내에는 2개의 절리 세트가 존재하는 것으로 가정하였다; 절리세트1은 20m간격의 56° 경사의 절리들로 구성되었고, 절리세트2는 절리세트1에 수직방향으로 20m간격의 34° 경사의 절리들로 구성되었다. 해석은 2차원 해석 코드인 UDEC을 사용하였다. 특히 공동 주변 절리에서의 거동변화를 파악하기 위하여 Barton-Bandis 절리 모델을 사용하였고, PWR 사용후 핵연료로부터의 시간의존 방사성 붕괴열 영향 분석 및 steady state 유동 알고리즘을 이용한 수리해석을 하였다.

주요어 : 방사성폐기물 처분장, 화강암, 사용후 핵연료, 열수리역학적 연성거동, 절리

The objective of this present study is to understand long term(500 years) thermohydromechanical interaction behavior on joints adjacent to a repository cavern, when high level radioactive wastes are disposed of within discontinuous granitic rock masses, and then, to contribute this understanding to the development of a disposal concept. The model includes a saturated discontinuous granitic rock mass, PWR spent nuclear fuels in a disposal canister surrounded with compacted bentonite inside a deposition hole, and mixed bentonite backfilled in the rest of the space within a repository cavern. It is assumed that two joint sets exist within a model. Joint set 1 includes joints of 56° dip angle, spaced 20m apart, and joint set 2 is in the perpendicular direction to joint set 1 and includes joints of 34° dip angle, spaced 20m apart. The two dimensional distinct element code, UDEC is used for the analysis. To understand the joint behavior adjacent to the repository cavern, Barton-Bandis

* Corresponding author: njwkim@kaeri.re.kr

joint model is used. Effect of the decay heat from PWR spent fuels on the repository model has been analyzed, and a steady state flow algorithm is used for the hydraulic analysis.

Key words : radwaste repository, granite, spent fuel, thermohydromechanical interaction behavior, joint

Introduction

High level radioactive wastes are disposed at a location very deep underground in a rock mass in order to isolate high level radioactive materials from man and his environment. The principle of a deep geological disposal is to isolate wastes from the biosphere by multiple barriers. A rock mass is the most important isolation barrier, especially granite being the most common and important repository host rock.

Granite masses are generally fractured in preferred orientations, and the degree of fracturing decreases with increased depth. The matrix of a granitic rock mass is practically impermeable with a very low hydraulic conductivity. Hence, groundwater flows almost exclusively through the fractures. Hydraulic conductivity of a granitic rock mass depends on the degree of fracturing and on the interconnections between the fractures. Mechanical stability is high and depends on the crystal size, degree of stratification, and mineral composition. The response to mechanical loading can be characterized as brittle and nonplastic. The high strength of granitic rock enables high stability in underground openings in rock masses. Thermal expansion of granite is low. However, thermal stresses may lead to microcracking due to different thermal expansions of rocks and water inclusions. Thermal conductivity of granite is moderately good and rather independent from the temperature.

An underground cavern represents a region of stress release causing mechanical deformations and of pressure drop inducing groundwater flow. For hard crystalline granitic rocks and in the presence of preexisting joints, mechanical effects are concentrated at joints. Redistribution of a local stress field around a cavern may result in instability and release of rock blocks from a cavern wall into a cavern opening. As excavation proceeds, rock responds mechanically and joints in the vicinity of a cavern are compressed to a smaller aperture value. Since mechanical compression rate is higher than groundwater drainage rate, groundwater pressure builds up. This then decays after completion of a cavern and mechanical compression stabilized, and then groundwater is allowed to drain from joints.

The assessment of coupling effects of rock mass stability, groundwater flow through a repository, external stresses, and thermal effects is an important part in the safety evaluation of a disposal system. The prediction of this coupled phenomena is also very important in planning and designing an underground opening in rock masses with discontinuities, such as fractures and faults, which show a significant effect on this coupled behavior.

State of the art studies on various coupled processes for rock joints have been summarized by Tsang(1990). For coupled thermal and mechanical behavior, the distinct element method has been used to analyze the behavior of fractured rock masses for a radioactive waste repository(Shen et al,1990). For coupled hydraulic and thermal behavior, the effect of increasing temperature, due to the decay heat

from high level radioactive wastes, on the groundwater flow around the repository has been studied by many researchers(Hart,1981;Noorishad et al, 1984). For coupled hydraulic, thermal, and mechanical behavior, Hart(1981) presented a model which fully describes the coupled behavior in nonlinear porous geological systems by an explicit finite difference method.

The objective of this present study is to understand long term(500 years) thermohydromechanical coupling behavior on joints in the vicinity of a repository cavern, and then, to contribute this understanding to the development of a high level radioactive waste disposal concept.

Numerical model

1. High-level radioactive waste repository

High level radioactive wastes considered in this study are the PWR spent fuels cooled for the period of 40 years. Four assemblies of PWR spent fuels are placed in a hollow corrosion resistant cylindrical canister, and then, fixed with a cast iron insert between the fuel assemblies and the canister.

The repository cavern is to be located deep underground in a granitic rock mass with discontinuities. The caverns are 250m long, spaced 40m apart, 6m wide, and have a vertical wall height of 4.5m and an arch shaped roof with a crown 7m above the cavern floor. Vertical deposition holes, with a diameter of 2.24m and a length of 7.83m, are located beneath the cavern floor along the centerline of the cavern at a pitch of 6m. PWR spent fuels contained in a cylindrical canister are vertically placed in each deposition hole. Then, compacted bentonite buffer material fills the area between the canister and the surrounding rock mass, and backfill material, a mixture of bentonite and crushed rock, fills the rest of the space inside the cavern(Fig. 1).

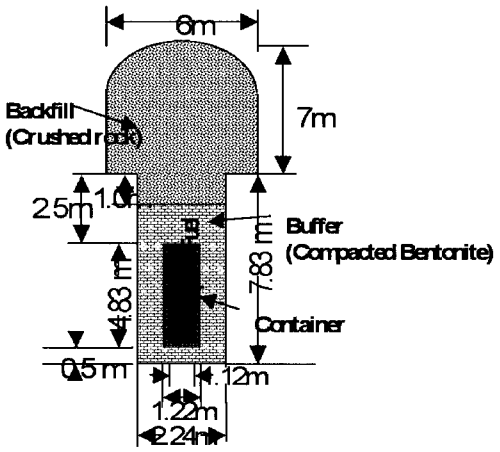

Fig. 1. A cavern and a deposition hole with a canister

Radioactive materials in PWR spent fuels generate decay heat through a radioactive decay process. The decay heat generated will influence the surroundings, such as canisters, buffer and backfill materials, groundwater flow, adjacent rock mass, and the biosphere. Therefore, the behavior of the repository system should be analyzed for the stability under the decay heat generated, H(T) in w/tHM;

$$H(T)= 2201169e^{-5.205T}+1693.22e^{-0.018T} +124.7e^{-0.00058T}+19.134e^{-0.000042T} +1.429e^{-0.000001T} \quad (1)$$

where, T is the time after discharging PWR spent fuels, $0 \leq T \leq 106$ years(Kang,2000).

2. Modeling

A 200m repository model shown in Figs. 2, 3, and 4 is to simulate long term(500 years) thermohydromechanical interaction behavior of the repository.

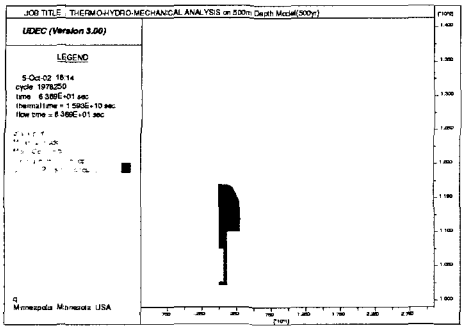

Fig. 2. Enlarged view of a repository model showing a tunnel and a deposition hole with a canister

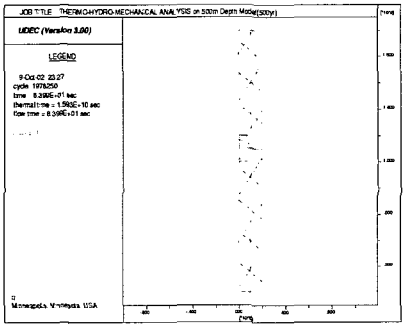

Fig. 3. A 200m repository model with joints

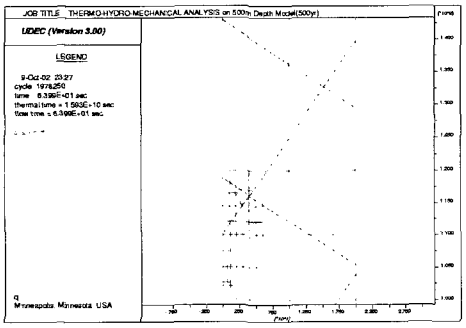

Fig. 4. Enlarged view of a 200m repository model with joints

There are two joint sets in the repository model; joint set 1 is 56° dip joints spaced 20m apart, and joint set 2 is 34° dip joints spaced 20m apart which are in the perpendicular direction to joint set 1.

A symmetry in the repository layout of multiple caverns in parallel with equal spacing has been utilized in modeling in order to simplify the analysis. Horizontal boundaries are assumed to be far enough from heat generating wastes on the top and the bottom of the model. Excavation of caverns, emplacement of wastes, and filling of buffer materials are all assumed to be instantaneous, and horizontal and vertical stresses are assumed to be equal initially.

Granitic rock mass is assumed to be homogeneous and isotropic satisfying Mohr-Coulomb's elastoplastic failure criteria, and compacted and mixed bentonites are regarded as elastoplastic material satisfying Drucker-Prager's failure criteria. The material for the canister is assumed to be homogeneous, isotropic, and linearly elastic. Barton-Bandis joint constitutive model is used for rock joints(Itasca, 1996).

In order to do a two dimensional approximation using the UDEC code, discrete waste location is distributed uniformly along the disposal cavern. This means that a heat generating trench is located below the cavern floor along the centerline of the disposal cavern. After the consideration of the tributary heating area of $10{,}000m^2$ which is equal to the area of a cavern length of 250m multiplied by a cavern spacing of 40m, heat flux, F, is then obtained from the equation (1),

$$F=(28.0554)e^{-(5.708E-10)t}+(4.1492)e^{-(1.839E-11)t} +(0.6486)e^{-(1.332E12)t}+(0.04876)e^{-(3.171E-14)t} \quad (2)$$

where, t is the time after 40 years of cooling, $0 \leq t \leq 3.1536E13$ sec, F in w/m2.

For the hydraulic analysis using a steady state flow algorithm, groundwater flows through discontinuities in a rock mass. A fully coupled

hydromechanical analysis is performed in which fracture conductivity is dependent on the mechanical deformation of a joint aperture; conversely, joint water pressures affect the mechanical behavior. Groundwater flow is governed by the pressure differential between adjacent domains. The cubic law for flow in a planar fracture is used in UDEC(Itasca,1996). The flow rate, q, from a domain with pressure p1 to a domain with pressure p_2 is given by

$$q = -k_j a^3(\Delta p/l) \quad (3)$$

where k_j is a joint permeability factor whose theoretical value is $(1/12\mu)$, μ is the dynamic viscosity of the fluid, a is the contact hydraulic aperture, and l is the length assigned to the contact between the domains.

$$\Delta p = p_2 - p_1 + \rho_w g(y_2 - y_1) \quad (4)$$

where ρ_w is the fluid density, g is the acceleration of gravity, and y_1, y_2 are the y-coordinates of domain centers.

The hydraulic aperture is given by

$$a = a_o + u_n \quad (5)$$

where a_o is the joint aperture at zero normal stress, and u_n is the joint normal displacement.

For the thermal analysis, this model simulates transient heat conduction in materials and the subsequent development of thermally induced displacements and stresses. Heat transfer is modeled as isotropic conduction and heat decays exponentially with time. The thermal analysis in UDEC (Itasca, 1996) provides only one-way coupling to the mechanical stress calculation through a thermal expansion coefficient and to the calculation for groundwater flow in joints through the temperature dependency of groundwater density and joint permeability. The basic equation of conductive heat transfer is Fourier's law.

$$Qi = -k_{ij}(\partial T/\partial x_j) \quad (6)$$

where Q_i is the flux in the i-direction, kij is the thermal conductivity tensor, and T is the temperature. The change in temperature for any mass is as follows,

$$(\partial T/\partial t) = Q_{net}/(C_p M) \quad (7)$$

where Q_{net} is the net heat flow into mass, C_p is the specific heat, and M is the mass.

The equations (6) and (7) are the basis of the thermal version of UDEC. Temperature changes cause stress changes,

$$\Delta\sigma_{ij} = -\delta_{ij}\, 3\, K^* \alpha\ \Delta T \quad (8)$$

where $\Delta\sigma_{ij}$ is the change in stress σ_{ij}, δ_{ij} is the Kronecker delta, K^* is K(for plane strain) and is equal to 6KG/(3K+4G) for plane stress, K is the bulk modulus, G is the shear modulus, α is the linear thermal expansion coefficient, and ΔT is the temperature change.

3. Initial and boundary conditions

Due to the symmetry in the repository layout of multiple caverns in parallel with equal shape, length, and spacing, half of the repository is used in the model, and symmetric boundary conditions are used. Boundary conditions for this fully saturated 200m model are fixed horizontal displacements on both sides, fixed vertical displacement at the bottom, and free at the surface. Impermeable boundary conditions are assumed on both sides and at the bottom of the model.

For thermal boundary conditions, it is assumed to be adiabatic on both sides and at the bottom.

Table 1. Mechanical and thermal properties of granite, compacted and mixed bentonite, and canister cast iron insert

Parameter	Granite	Compacted bentonite	Mixed bentonite	Canister cast iron insert
Density, kg/m^3	2700.0	2100.0	2100.0	8000.0
Bulk modulus, Gpa	40.0	3.5	3.33	167.0
Shear modulus, Gpa	24.0	0.75	1.54	77.0
Thermal conductivity, W/mC	3.2	1.2	2.0	15.2
Thermal expansion coefficient, 1/°C	8.3E-6	0.0	8.3E-6	8.2E-6
Specific heat, J/kgC	815.0	1000.0	800.0	504.0
Friction angle, °	25.0			
Cohesion, Mpa	16.0			
Dilation	8.0			

Table 2. Mechanical properties of a joint set 1(56° dip angle) and a joint set 2(34° dip angle)

Param eter	Joint set 1	Joint set 2
Joint normal stiffness, Gpa/m	1.6E14	2.0E14
Joint shear stiffness, Gpa/m	2.0E13	2.3E13
Joint cohesion, Mpa	0.3	0.1
Joint dilation, °	0.0	0.0
Joint aperture, m	2.5E-3	1.0E-3
Joint permeability, 1/(Pa*sec)	1.0	3.0
Joint residual aperture, m	5.0E-5	5.0E-5
Joint roughness coefficient	7.0	5.0
Joint compressive strength, Mpa	30.0	30.0
Residual angle of friction, °	30.0	28.0
Intact rock compressive strength, Mpa	150.0	150.0

The temperature is assumed to be 20°C at ground surface and to increase by 0.6°C for every 20m below the surface. Therefore, the initial temperature is 32°C at the top and 38°C at the bottom of the model.

4. Material properties

Material properties for the host granitic rock, rock joint, compacted and mixed bentonite, and canister cast iron insert are shown in Tables 1 and 2(Kang et al,2000; Hokmark et al,1991;

Hokmark,1990; Johansson et al,1991; SKB,1997; SKB,1997).

Joint behavior in a 500m depth model with two joint sets

A 200m repository model located within a discontinuous rock mass at a depth of 500m is analyzed to understand long term (500 years) thermohydromechanical interaction behavior on joints adjacent to the repository cavern.

The model includes a saturated discontinuous granitic rock mass, PWR spent nuclear fuels in a disposal canister surrounded with compacted bentonite inside the deposition hole, and mixed bentonite backfilled in the rest of the space within the repository cavern. There are two joint sets within a model. Joint set 1 includes joints of the 56° dip angle, spaced 20m apart, and joint set 2 is in the perpendicular direction to joint set 1 and includes joints of 34° dip angle, spaced 20m apart.

The two dimensional distinct element code, UDEC is used for the analysis. To understand the joint behavior adjacent to the repository cavern, Barton-Bandis joint model is used. Effect of the decay heat from PWR spent fuels on the repository model has been analyzed, and a steady state flow algorithm is used for the hydraulic analysis.

1. Initial stage

Insitu stresses are calculated, and then used for the next analyses, but displacements calculated are reset to zero values before the start of the next analyses. Distributions of vertical and horizontal components of insitu stresses are shown in Figs. 5 and 6.

The insitu stresses on the 500m depth model are in the range from 11MPa at the top to 16MPa at the bottom of the model.

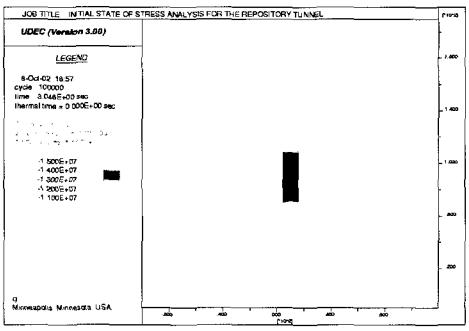

Fig. 5. Distribution of a vertical component of an insitu stress on a 500m depth repository model

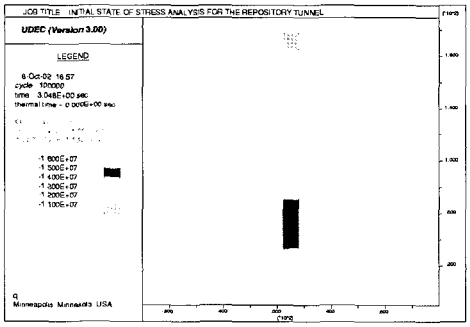

Fig. 6. Distribution of a horizontal component of an insitu stress on a 500m depth repository model

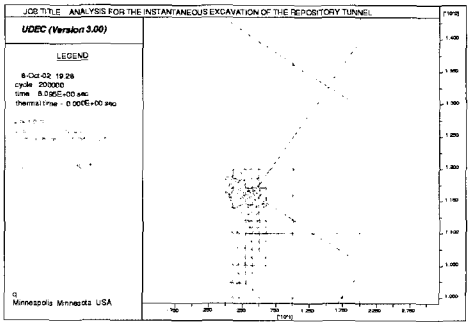

Fig. 7. Enlarged view of the displacement distribution on a repository model after an Instantaneous tunnel excavation

2. After an instantaneous excavation

After an instantaneous excavation, displacement and principal stress distributions in the vicinity of the repository cavern are shown in Figs. 7 and 8.

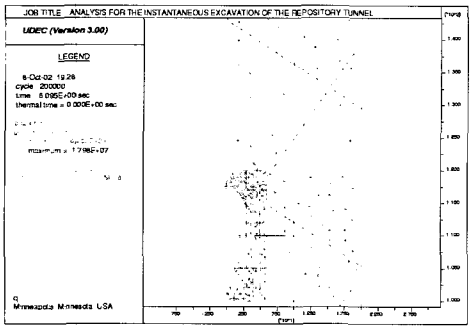

Fig. 8. Enlarged view of the principal stress distribution on a repository model after an instantaneous tunnel excavation

Maximum displacement is 50.4mm directed horizontally toward the excavated space and occurs at the cavern roof-wall intersection. The cavern crown displaces 19.2mm downward upon excavation. The stresses are concentrated in the vicinity of the cavern after an excavation. Minimum and maximum principal stresses near the cavern crown are 60.3MPa and 10.2MPa, and near the cavern floor-wall intersection are 20.28MPa and 6.82MPa, in that order.

Maximum displacements and stresses on the 56° dip joint passing through the cavern roof-wall intersection are summarized in Table 3. Maximum vertical displacement of 4.8mm occurs at the other end of the joint away from the cavern, and maximum horizontal displacement of 20.5mm occurs at the cavern roof-wall intersection.

Maximum vertical stress is 49.06MPa and occurs at the cavern crown level on the joint, and maximum horizontal stress is 17.19MPa and occurs at the other end zone away from the cavern. Maximum shear stress of 2.66MPa occurs near the cavern roof-wall intersection.

Table 3. Results on a joint of 56° dip angle passing through a cavern roof-wall intersection of a repository model

Results	After an instantaneous excavation	After placing canisters and buffer filling	After 500 years from waste emplacement
Max. vertical displacement(mm)	-4.8	-5.5	60.5
Max. horizontal displacement(mm)	-20.5	-21.7	-29.0
Max. vertical stress(MPa)	-49.06	-43.51	-17.46
Max. horizontal stress(MPa)	-17.19	-16.34	-36.63
Max. shear stress(MPa)	2.66	2.89	2.46

Table 4. Hydraulic aperture variations on the joint of 56° dip angle passing through a cavern roof-wall intersection in four different stages: at an initial stage, after an instantaneous excavation, after placing canisters and buffer filling, and after 500 years from waste emplacement

Point coordinates(m,m)	Hydraulic aperture(m) at an initial stage	Hydraulic aperture(m) after an instantaneous excavation	Hydraulic aperture(m) after placing canisters and buffer filling	Hydraulic aperture(m) after 500 years from waste emplacement
4.0,116.0	7.2E-4	7.4E-4	7.5E-4	4.4E-3
4.03,116.03	9.0E-4	7.6E-3	7.7E-3	4.3E-4
4.09,116.12	4.3E-4	7.4E-4	4.3E-4	4.3E-4
4.73,117.07	9.0E-4	2.2E-3	5.0E-4	4.3E-4
5.0,117.4	9.0E-4	2.3E-3	2.3E-3	7.0E-4
6.0,119.0	9.0E-4	9.0E-4	1.4E-3	3.0E-3
6.75,120.0	5.9E-4	4.3E-4	4.3E-4	4.3E-4
10.0,125.0	4.3E-4	4.3E-4	4.3E-4	1.7E-3
15.25,132.7	4.3E-4	4.3E-4	4.3E-4	4.3E-4

Hydraulic aperture variations on the 56° dip joint are shown in Table 4.

The hydraulic aperture at the coordinate of (4.0m, 116.0m) is 7.2E-4m at an initial stage, and changes slightly to 7.4E-4m after an instantaneous excavation, but that at the coordinate of (4.03m, 116.03m) is initially 9.0E-4m and then becomes 7.6E-3m after an excavation which is 8 times bigger than the

initial value.

The hydraulic aperture at the coordinate of (5.0m,117.4m) is 2.3E-3m after an excavation which is 2.5 times bigger than the initial value of 9.0E-4m.

The hydraulic apertures along the joint from the coordinate of (10.0m, 125.0m) to the other end of the joint stay constant and are 4.3E-4m. Hydraulic aperture, normal and shear displacements, and normal stress distributions along the line of the 56° dip joint are shown in Figs. 9-12.

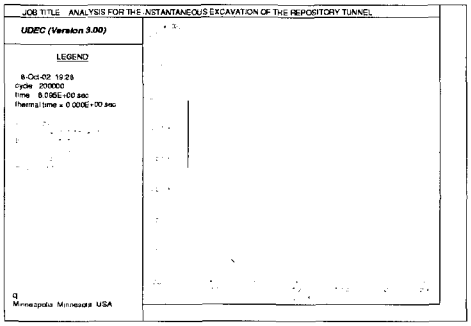

Fig. 9. Hydraulic aperture variation along the line of a 56° dip joint passing through a tunnel roof-wall intersection after an instantaneous excavation

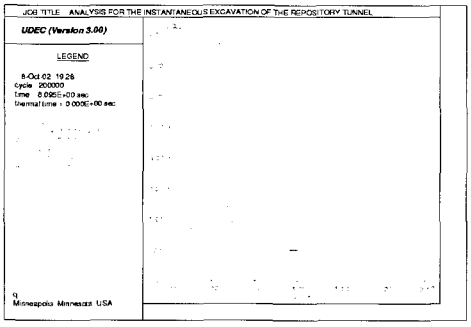

Fig. 10. Normal displacement distribution along the of a 56° dip joint passing through a tunnel roof-wall intersection after an instantaneous excavation

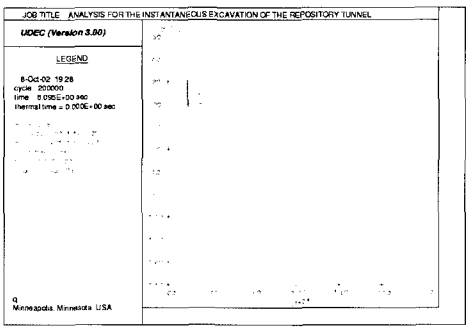

Fig. 11. Shear displacement distribution along the line of a 56° dip joint passing through a tunnel roof-wall intersection after an instantaneous excavation

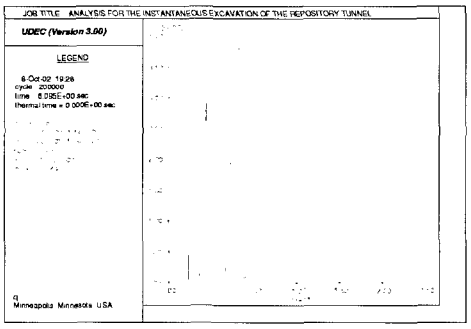

Fig. 12. Normal stress distribution along the line of a 56° dip joint passing through a tunnel roof-wall intersection after an instantaneous excavation

They all show large variations in the region from the cavern wall to a radial distance away horizontally, and small variations in the next region to a diameter distance away horizontally, and then, stay fairly constant beyond that region. Maximum displacements and stresses on the 34° dip joint passing slightly above the cavern crown are summarized in Table 5.

Maximum vertical displacement of 16.9mm occurs near the cavern crown, and horizontal displacements are zero along the line of the joint. Maximum vertical and horizontal stresses are, in

turn, -15.52MPa at the other end of the joint away from the cavern and 3.43MPa near the cavern crown. Maximum shear stress of 5.41MPa occurs at the other end away from the cavern.

Table 5. Results on a joint of 34° dip angle passing slightly above a cavern crown of a repository model

Results	After an instantaneous excavation	After placing canisters and buffer filling	After 500 years from waste emplacement
Max. vertical displacement(mm)	-16.9	-18.9	40.47
Max. horizontal displacement(mm)	0.0	0.0	-33.98
Max. vertical stress(MPa)	-15.52	-14.2	-27.22
Max. horizontal stress(MPa)	3.43	3.4	-38.69
Max. shear stress(MPa)	-5.41	-5.3	-6.21

Table 6. *Hydraulic aperture variations on the* joint of 34° dip angle passing slightly above a cavern crown in four different stages: at an initial stage, after an instantaneous excavation, after placing canisters and buffer filling, and after 500 years from waste emplacement

Point coordinates(m,m)	Hydraulic aperture(m) at an initial stage	Hydraulic aperture(m) after an instantaneous excavation	Hydraulic aperture(m) after placing canisters and buffer filling	Hydraulic aperture(m) after 500 years from waste emplacement
0.0,118.8	4.3E-4	7.7E-3	8.6E-3	1.2E-2
0.53,118.44	4.3E-4	3.9E-3	4.7E-3	6.6E-3
1.09,118.07	9.0E-4	2.3E-3	2.5E-3	2.8E-3
1.56,117.75	4.3E-4	4.3E-4	4.3E-4	5.0E-4
1.99,117.45	7.1E-4	7.5E-4	7.5E-4	2.8E-3
2.69,116.98	9.0E-4	6.1E-3	6.4E-3	8.0E-3
3.0,116.78	9.0E-4	7.5E-4	7.5E-4	4.7E-3
3.94,116.14	9.0E-4	4.3E-4	4.3E-4	4.3E-4
4.05,116.07	9.0E-4	4.3E-4	4.3E-4	1.5E-2
4.97,115.44	7.1E-4	4.3E-4	4.3E-4	4.3E-4
6.0,114.75	9.0E-4	4.3E-4	4.3E-4	4.3E-4

Hydraulic aperture variations on the 34° dip joint are shown in Table 6.

The hydraulic aperture at the coordinate of (0.0m,118.8m) is 4.3E-4m at an initial stage, but that after an excavation is 7.7E-3m which is 18 times bigger than the initial value.

The hydraulic aperture at the coordinate of (2.69m, 116.98m) is 6.1E-3m which is 7 times bigger than the initial 9.0E-4m. From this location to the other end of the joint, the hydraulic apertures stay fairly constant.

Hydraulic aperture, normal and shear displacements, and normal stress distributions along the line of the 34° dip joint are shown in Figs. 13-16.

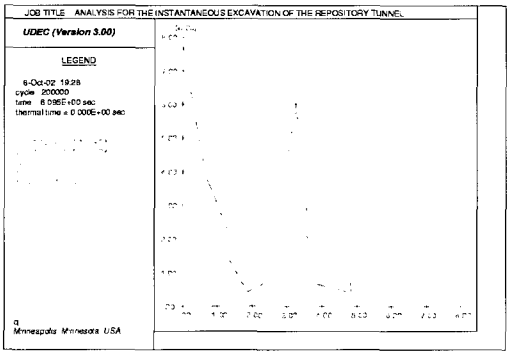

Fig. 13. Hydraulic aperture variation along the line of a 34° dip joint passing through a tunnel crown after an instantaneous excavation

They all show large variations in the region from the cavern wall to a radial distance away horizontally, and small variations in the next region to a diameter distance away horizontally from the cavern wall, and then, stay fairly constant beyond that region.

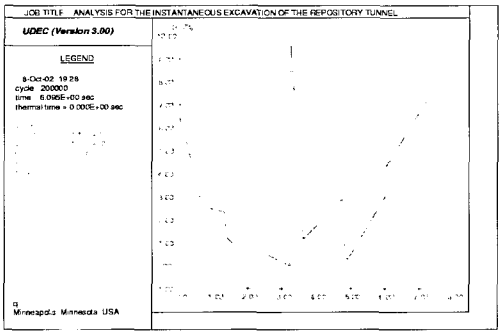

Fig. 14. Normal displacement distribution along the line of a 34° dip joint passing through a tunnel crown after an instantaneous excavation

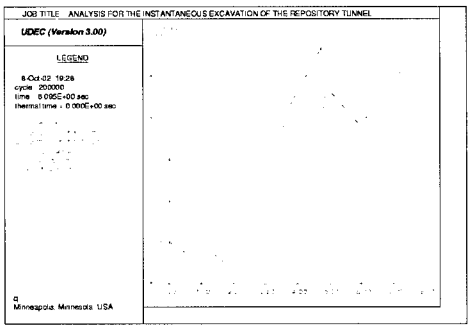

Fig. 15. Shear displacement distribution along the line of a 34° dip joint passing through a tunnel crown after an instantaneous excavation

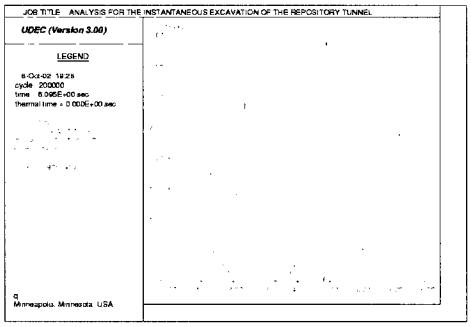

Fig. 16. Normal stress distribution along the line of a 34° dip joint passing through a tunnel crown after an instantaneous excavation

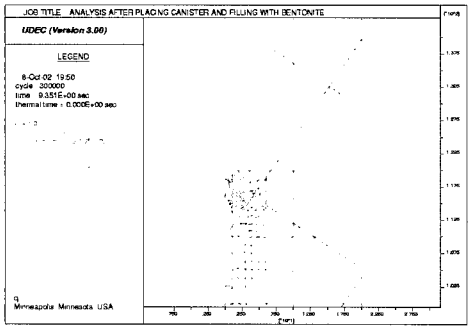

Fig. 17. Displacement distribution on a repository model after placing canisters and buffer filling

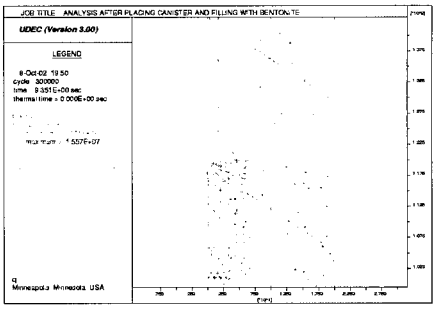

Fig. 18. Principal stress distribution on a repository model after placing canisters and buffer filling

3. After waste emplacement and buffer filling

After waste emplacement and buffer filling, displacement and principal stress distributions in the vicinity of the repository model are shown in Figs. 17 and 18.

Maximum displacement is 51.6 mm directed toward the backfilled cavern, and occurs at the cavern roof-wall intersection, and the cavern crown displaces 21.2mm downward. Minimum and maximum principal stresses near the cavern crown are, in turn, 55.58 MPa and 11.09 MPa, and near the cavern floor-wall intersection are 22.09 MPa and 6.26 MPa, respectively.

Maximum displacements and stresses on the 56° dip joint passing through the cavern roof-wall intersection are summarized in Table 3.

Maximum vertical displacement of 5.5mm occurs at the other end zone of the joint away from the cavern, and maximum horizontal displacement of 21.7 mm occurs at the cavern roof-wall intersection. Maximum vertical stress is 43.51 MPa and occurs at the cavern crown level on the joint, and maximum horizontal stress is 16.34 MPa and occurs at the other end zone away from the cavern. Maximum shear stress of 2.89 MPa occurs near the mid location on the joint. Hydraulic aperture variations on the 56° dip joint are shown in Table 4.

The hydraulic aperture at the coordinate of (4.0m, 116.0m) is 7.5E-4m after waste emplacement and buffer filling, but that at the coordinate of (4.03m, 116.03m) is 7.7E-3m. The hydraulic aperture at the coordinate of (6.0m,119.0m) is 1.4E-3m. The hydraulic apertures along the joint from the coordinate of (6.75m,120.0m) to the other end of the joint stay constant and are 4.3E-4m. Hydraulic aperture, normal and shear displacements, and normal stress distributions along the line of the 56° dip joint are shown in Figs. 19-22.

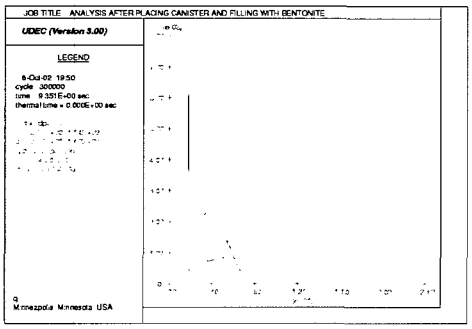

Fig. 19. Hydraulic aperture variation along the line of a 56° dip joint passing through a tunnel roof-wall intersection after placing canisters and buffer filling

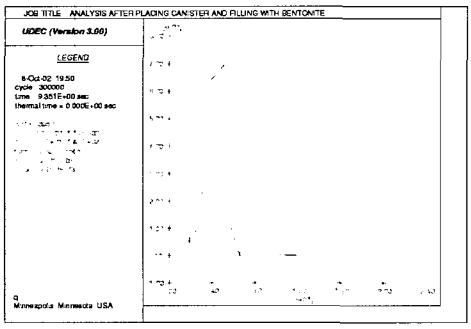

Fig. 20. Normal displacement distribution along the line of a 56° dip joint passing through a tunnel roof-wall intersection after placing canisters and buffer filling

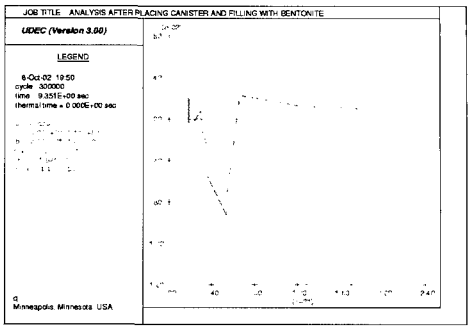

Fig. 21. Shear displacement distribution along the line of a 56° dip joint passing through a tunnel roof-wall intersection after placing canisters and buffer filling

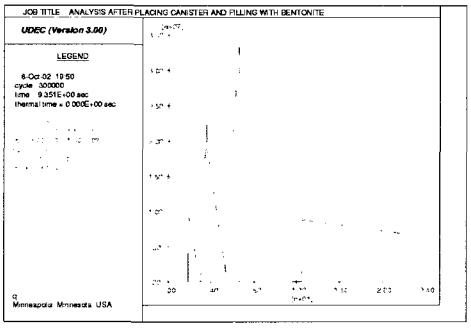

Fig. 22. Normal stress distribution along the line of a 56° dip joint passing through a tunnel roof-wall intersection after placing canisters and buffer filling

They all show large variations in the region from the cavern wall to a radial distance away horizontally, and small variations in the next region to a diameter distance away horizontally from the cavern wall, and then, stay fairly constant beyond that region.

Maximum displacements and stresses on the 34° dip joint passing slightly above the cavern crown are summarized in Table 5.

Maximum vertical displacement of 18.9mm occurs near the cavern crown, and horizontal displacements are zero along the line of the joint.

Maximum vertical and horizontal stresses are, in turn, -14.2 MPa and 3.4 MPa, and occur at the other end of the joint away from the cavern. Maximum shear stress of 5.3 MPa occurs at the other end of the joint away from the cavern. Hydraulic aperture variations on the 34° dip joint are shown in Table 6.

The hydraulic aperture at the coordinate of (0.0m,118.8m) is 8.6E-3m. The hydraulic aperture at the coordinate of (3.0m,116.78m) is 7.5E-4m. From this location to the other end of the joint away from the cavern, the hydraulic apertures stay fairly constant. Hydraulic aperture, normal and shear displacements, and normal stress distributions along the line of the 34° dip joint are shown in Figs. 23~26.

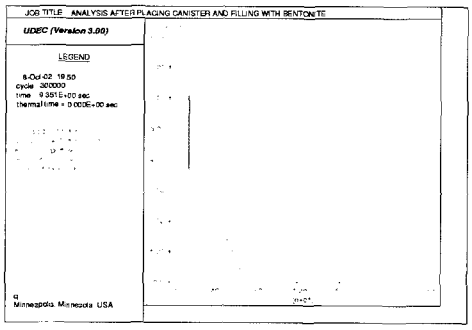

Fig. 23. Hydraulic aperture variation along the line of a 34° dip joint passing through a tunnel crown after placing canisters and buffer filling

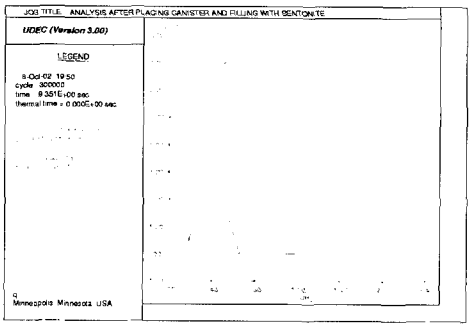

Fig. 24. Normal displacement distribution along the line of a 34° dip joint passing through a tunnel crown after placing canisters and buffer filling

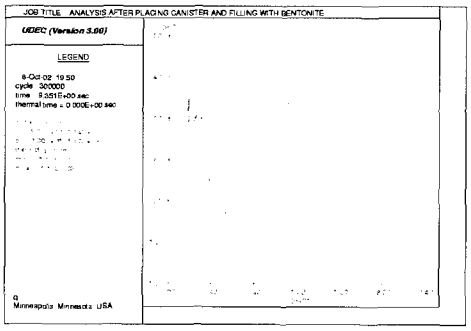

Fig. 25. Shear displacement distribution along the line of a 34° dip joint passing through a tunnel crown after placing canisters and buffer filling

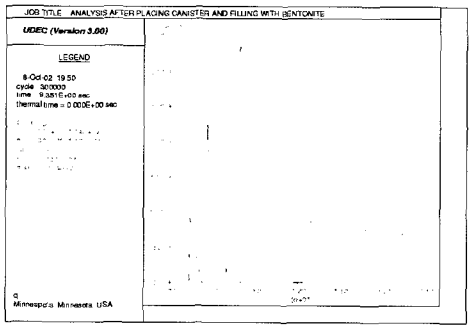

Fig. 26. Normal stress distribution along the line of a 34° dip joint passing through a tunnel crown after placing canisters and buffer filling

They all show large variations in the region from the cavern wall to a radial distance away horizontally, and small variations in the next region to a diameter distance away horizontally from the cavern wall, and then, stay fairly constant beyond that region.

There are not much differences in the behavior of joints in stages after an instantaneous excavation and after waste emplacement and buffer filling.

4. Long term behavior after waste emplacement

A repository model with two joint sets in a granitic rock mass at a depth of 500m is analyzed to understand the behavior of the joint adjacent to the repository subjected to a thermohydromechanical interaction. The displacement and principal stress distributions in the vicinity of the repository model after 500 years from waste emplacement are shown in Figs. 27 and 28.

Displacement of 40.3mm occurs at the cavern crown directed upward. Displacements at the floor center and at the bottom of the deposition hole are, in turn, 39.6mm and 49.1mm upward. Minimum and maximum principal stresses near the cavern crown are 58.61MPa and 13.47MPa, and near the cavern floor-wall intersection are 26.6MPa and 12.63MPa, in that order.

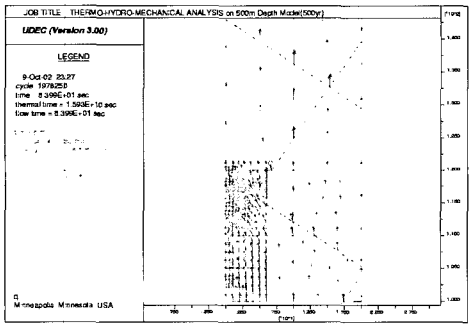

Fig. 27. Displacement distribution on a repository model after 500 years from waste emplacement

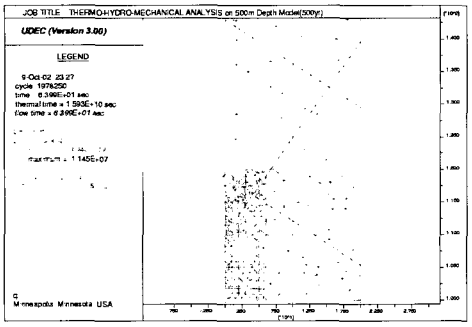

Fig. 28. Principal stress distribution on a repository model after 500 years from waste emplacement

Temperature histories at various locations along the horizontal line connecting the canister center on the repository model for the period of 500 years from waste emplacement are shown in Fig. 29.

The corresponding locations from the top in Fig. 29 are the canister center, canister surface, deposition hole wall, 2m, 3m, 4m, 5m, 6m, 10m, 15m, and 20m away from the canister center. The maximum temperatures at various locations mentioned above are 95.8° C, 95.2° C, 90.3° C, 87.8° C, 85.6° C, 84.0° C, 82.8° C, 81.9° C 79.8° C, 78.5° C, and 78.3° C, in that order. These maximum temperatures are reached after 30 to 100 years from waste emplacement. The temperature distributions at these locations after 500 years from waste emplacement are asymptotically reduced, and are in the range from 71° C to 76° C.

Vertical displacement histories at various locations around the cavern during the period of 500 years from waste emplacement are shown in Fig. 30. The corresponding locations from the top in Fig. 30 are the cavern floor-wall intersection, deposition hole-cavern floor intersection, cavern roof- wall intersection, cavern crown, canister center, canister surface center, cavern floor-wall intersection, and wall center of the deposition hole.

Vertical crown displacement is 3.7mm downward after 16 years, and then, shows a fast increase to a maximum displacement of 41.9mm upward after 200 years, and becomes 40.3mm upward after 500 years from waste emplacement. Vertical displacement histories at various locations around the cavern in Fig. 30 show similar behavior. Vertical displacements show fast increases for the first 200 years, and then, stay fairly constant for the rest of the period.

Maximum displacements and stresses on the

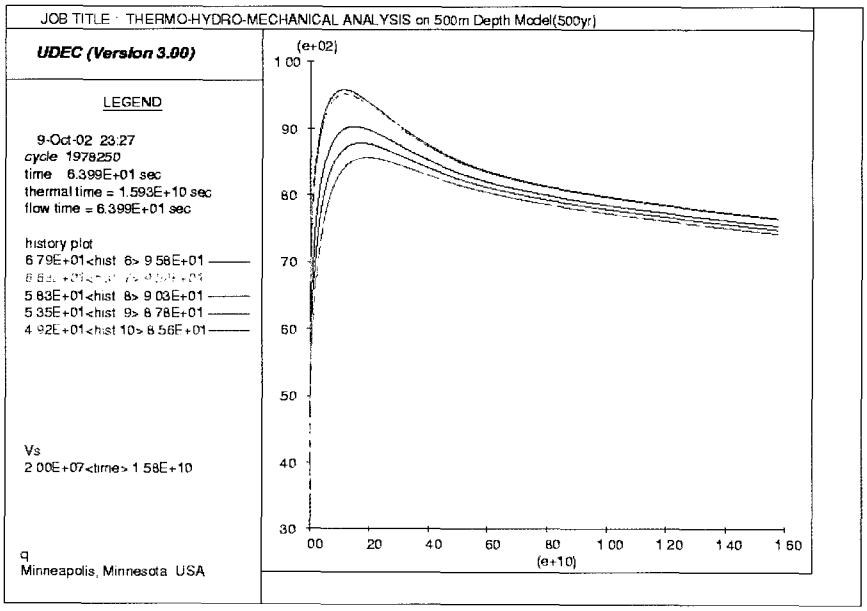

Fig. 29. *Temperature history at various locations along the horizontal line connecting the canister* center on a repository model for the period of 500 years from waste emplacement

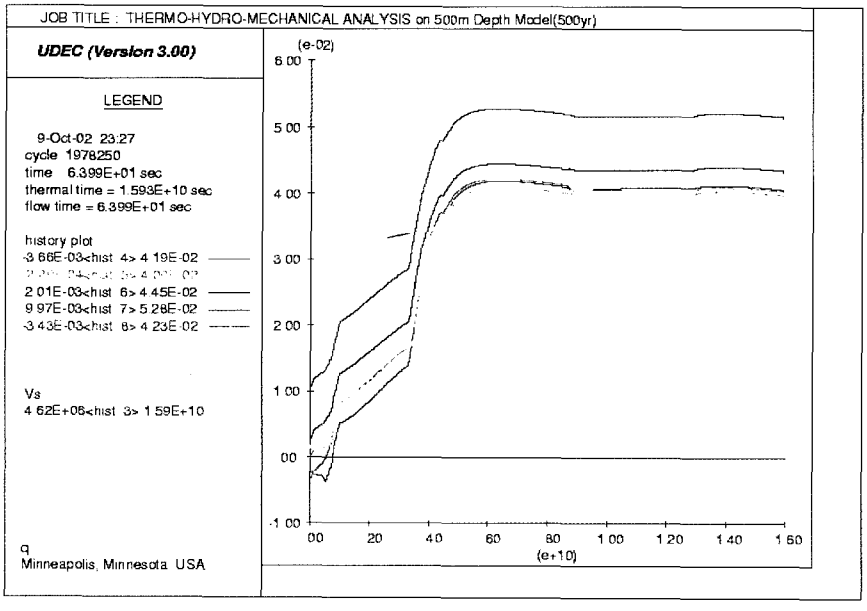

Fig. 30. Vertical displacement histories at various locations around a cavern during the period of 500 years from waste emplacement

56° dip joint passing through the cavern roof-wall intersection after 500 years from waste emplacement are shown in Table 3. Maximum vertical displacement is 60.5mm directed upward in the far end of the joint away from the cavern, and maximum horizontal displacement of 29.0mm directed toward the cavern occurs at the cavern roof-wall intersection.

Maximum vertical stress of 17.46 MPa occurs near the cavern roof-wall intersection, and maximum horizontal and shear stresses of 36.63MPa and 2.46MPa, in turn, occur at the far end of the joint away from the cavern. Hydraulic aperture variations on the 56° dip joint are shown in Table 4.

The hydraulic aperture at the coordinate of (4.0m, 116.0m) is 4.4E-3m after 500 years from waste emplacement which is 6 times bigger than that after waste emplacement and buffer filling. The hydraulic apertures at the coordinate of (6.0m, 119.0m) and (10.0m, 125.0m) are, in turn, 3.0E-3m and 1.7E-3m. The hydraulic apertures along the joint beyond the coordinate of (10.0m, 125.0m) to the other end of the joint stay constant and are 4.3E-4m. Hydraulic aperture, flow rate, and mean fluid velocity variations on the 56° dip joint after 500 years from waste emplacement are shown in Table 7.

Maximum flow rate is 1.0E-6m3/sec at the cavern roof-wall intersection, and maximum mean fluid velocity is 4.8E-4m/sec at the coordinate of (6.75m,120.0m). Hydraulic aperture, normal and shear displacements, normal stress, flow rate, and mean fluid velocity distributions along the line of the 56° dip joint are shown in Figs. 31-36.

They all show large variations in the region from the cavern wall to a radial distance away horizontally, and small variations in the next region to a diameter distance away horizontally from the cavern wall, and then, stay fairly constant beyond that region. Maximum displacements and stresses on the 34° dip joint passing slightly above the cavern crown are summarized in Table 5.

Maximum vertical displacement is 40.47mm and the distribution is fairly uniform.

Table 7. Variations of hydraulic aperture, flow rate, and mean fluid velocity on the joint of 56° dip angle passing through a cavern roof-wall intersection after 500 years from waste emplacement

Point coordinates (m,m)	Hydraulic aperture(m) after 500 years from waste emplacement	Flow rate(m^3/sec) after 500 years from waste emplacement	Mean fluid velocity(m/sec) after 500 years from waste emplacement
4.0,116.0	4.4E-3	1.0E-6	1.8E-4
4.03,116.03	4.3E-4	8.9E-9	2.0E-5
4.09,116.12	4.3E-4	8.9E-9	2.0E-5
4.73,117.07	4.3E-4	8.9E-9	2.0E-5
5.0,117.4	7.0E-4	2.7E-7	3.1E-4
6.0,119.0	3.0E-3	3.4E-7	1.5E-4
6.75,120.0	4.3E-4	2.1E-7	4.8E-4
10.0,125.0	1.7E-3	2.3E-7	2.3E-4
15.25,132.7	4.3E-4	3.0E-8	3.6E-4

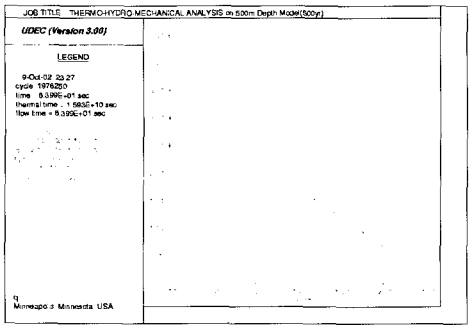

Fig. 31. Hydraulic aperture variation along the line of a 56° dip joint passing through a tunnel roof-wall intersection after 500 years from waste emplacement

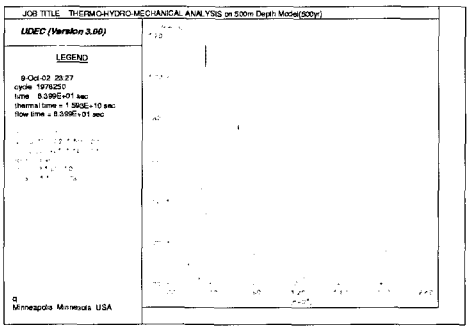

Fig. 34. Normal stress distribution along the line of a 56° dip joint passing through a tunnel roof-wall intersection after 500 years from waste emplacement

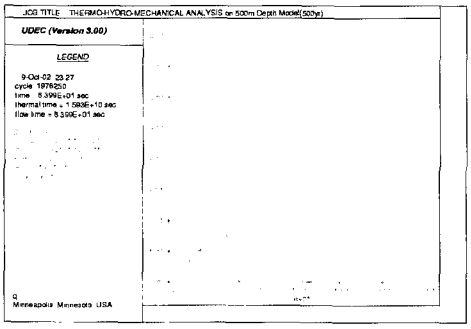

Fig. 32. Normal displacement distribution along the of a 56° dip joint passing through a tunnel roof-wall intersection after 500 years from waste emplacement

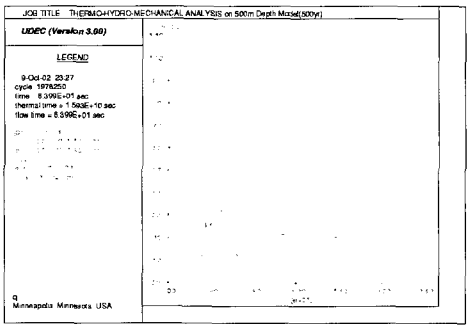

Fig. 35. Flow rate variations along the line of a 56° dip joint passing through a tunnel roof-wall intersection after 500 years from waste emplacement

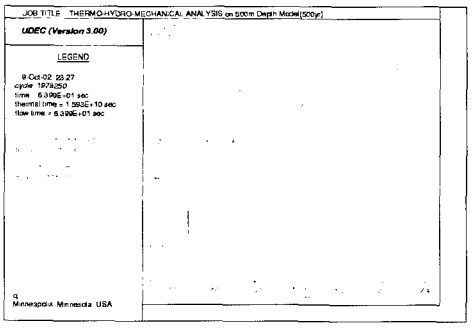

Fig. 33. Shear displacement distribution along the line of a 56° dip joint passing through a tunnel roof-wall intersection after 500 years from waste emplacement

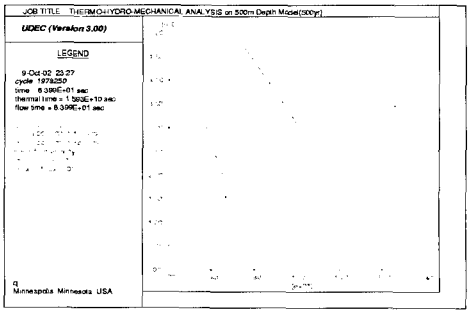

Fig. 36. Mean fluid velocity variations along the line of a 56° dip joint passing through a tunnel roof-wall intersection after 500 years from waste emplacement

Maximum horizontal displacement is 33.98mm and occurs at the cavern crown level on the joint. Maximum vertical and horizontal stresses are, in turn, -27.22 MPa and 38.69 MPa at the cavern crown level on the joint. Maximum shear stress of 6.21 MPa occurs at the other end zone away from the cavern.

Hydraulic aperture variations on the 34° dip joint are shown in Table 6. The hydraulic aperture at the coordinate of (0.0m,118.8m) is 1.2E-2m. The hydraulic aperture at the coordinate of (4.05m, 116.07m) is 1.5E-2m. From this location to the other end of the joint away from the cavern, the hydraulic apertures stay constant and are 4.3E-4m.

Hydraulic aperture, flow rate, and mean fluid velocity variations on the 34° dip joint after 500 years from waste emplacement are shown in Table 8.

Maximum flow rate of 1.7E-5 m^3/sec occurs at the coordinate of (3.94m, 116.14m), and maximum mean fluid velocity of 1.28E-3m/sec occurs at the coordinate of (1.56m, 117.75m). Hydraulic aperture, normal displacement, shear displacement, and normal stress distributions along the line of the 34° dip joint are shown in Figs. 37-42.

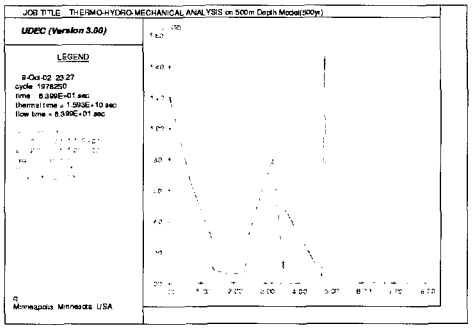

Fig. 37. Hydraulic aperture variation along the line of a 34° dip joint passing through a tunnel crown after 500 years from waste emplacement

They all show large variations in the region from the cavern wall to a radial distance away horizontally, and small variations in the next region to a diameter distance away horizontally from the cavern wall, and then, stay fairly constant beyond that region.

Table 8. Variations of hydraulic aperture, flow rate, and mean fluid velocity on the joint of 34° dip angle passing slightly above a cavern crown after 500 years from waste emplacement

Point coordinates(m,m)	Hydraulic aperture(m) after 500 years from waste emplacement	Flow rate(m^3/sec) after 500 years from waste emplacement	Mean fluid velocity(m/sec) after 500 years from waste emplacement
0.0,118.8	1.2E-2	0.0	0.0
0.53,118.44	6.6E-3	2.8E-6	4.2E-4
1.09,118.07	2.8E-3	2.0E-6	1.26E-3
1.56,117.75	5.0E-4	7.0E-7	1.28E-3
1.99,117.46	2.8E-3	3.0E-7	8.2E-4
2.69,116.98	8.0E-3	3.4E-6	3.2E-4
3.0,116.78	4.7E-3	5.0E-7	1.0E-4
3.94,116.14	4.3E-4	1.7E-5	1.26E-3
4.05,116.07	1.5E-2	3.0E-7	6.1E-4
4.97,115.44	4.3E-4	3.0E-7	6.1E-4
6.0,114.75	4.3E-4	2.0E-7	4.6E-4

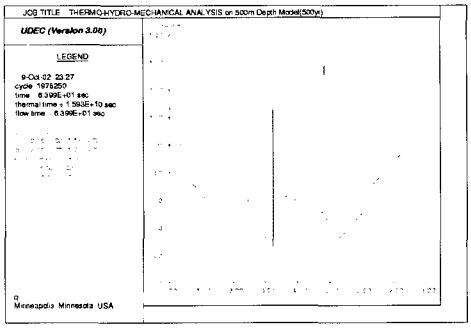

Fig. 38. Normal displacement distribution along the line of a 34° dip joint passing through a tunnel crown after 500 years from waste emplacement

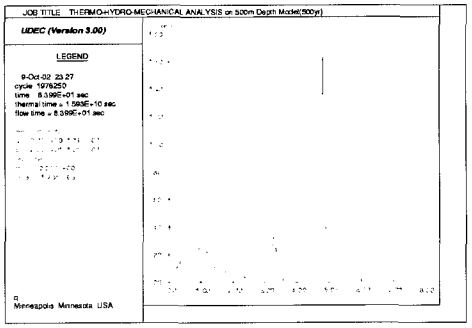

Fig. 41. Flow rate variations along the line of a 34° dip joint passing through a tunnel crown after 500 years from waste emplacement

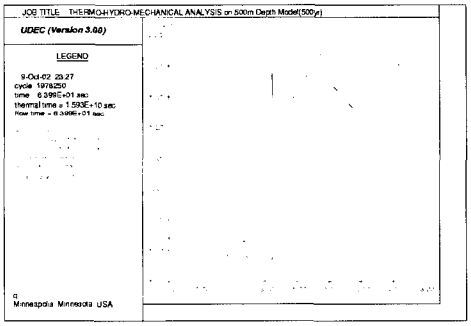

Fig. 39. Shear displacement distribution along the line of a 34° dip joint passing through a tunnel crown after 500 years from waste emplacement

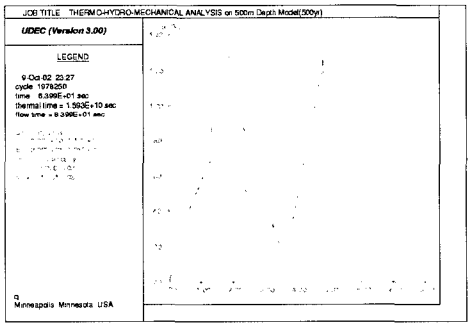

Fig. 42. Mean fluid velocity variations along the line of a 34° dip joint passing through a tunnel crown after 500 years from waste emplacement

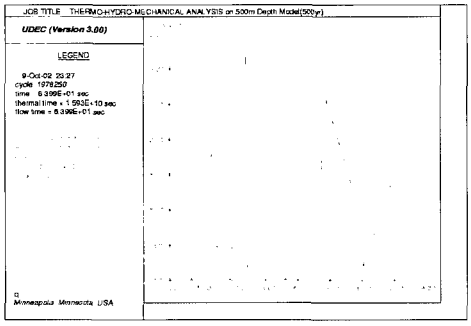

Fig. 40. Normal stress distribution along the line of a 34° dip joint passing through a tunnel crown after 500 years from waste emplacement

Conclusion

A 200m repository model, located at a depth of 500m in a saturated granitic rock mass with two joint sets, is analyzed to understand long term (500 years) thermohydromechanical interaction behavior on the joints adjacent to the repository cavern. To study the joint behavior in the vicinity of the repository cavern, Barton- Bandis joint model in the two dimensional distinct element code, UDEC is used. Effect of the decay

heat from PWR spent fuels on the repository model is analyzed, and a steady state flow algorithm is used for the hydraulic analysis.

Insitu stresses are calculated, and then used for the next analysis, but displacements calculated are reset to zero values before the start of the next analysis. After an instantaneous excavation, stresses are concentrated in the vicinity of the repository cavern, and the periphery of the repository cavern shows rather large displacements toward the excavated cavern.

Hydraulic aperture, normal and shear displacements, and normal stress distributions along the line of the 56° dip joint in Figs. 9-12 show large variations in the region from the cavern wall to a radial distance away horizontally, and small variations in the next region to a diameter distance away horizontally from the cavern wall, and then, stay fairly constant beyond that region. Hydraulic aperture, normal and shear displacements, and normal stress distributions along the line of the 34° dip joint in Figs. 23~26 show large variations in the region from the cavern crown to a radial distance away horizontally from the cavern wall, and stay fairly constant beyond that region.

The joint behavior after waste emplacement and buffer filling does not differ much from that after an instantaneous excavation.

For the long term (500 years) thermohydro-mechanical interaction behavior after waste emplacement and buffer filling, maximum temperatures at various locations along the horizontal line connecting the canister center on the repository model are in the range from 95.8° C to 78.3° C. These maximum temperatures are reached after 30 to 100 years after waste emplacement, The temperature distributions at these locations after 500 years from waste emplacement are asymptotically reduced, and are in the range from 71° C to 76° C.

Vertical displacement histories at various locations around the cavern during the period of 500 years from waste emplacement show that vertical displacements increase fast for the first 200 years, and then, stay fairly constant for the rest of the period.

The changes in displacements and stresses in the vicinity of an underground cavern cause deformation and stress changes in joints adjacent to the cavern. Normal and shear displacements, and normal stress distributions in joints adjacent to the cavern show large variations in the region from the cavern wall to a radial distance away horizontally, and small variations in the next region to a diameter distance away horizontally from the cavern wall, and then, stay fairly constant beyond that region. Normal and shear deformations in joints cause changes in joint aperture. Joint aperture is increased by an expansion due to a shear deformation, and is in a reciprocal proportion to normal stresses acting on joints. The changes in joint aperture cause joint permeability changes, and consequently have influences on the groundwater flow rate.

Acknowledgement

The present study is financially supported by the National Long Term Nuclear R&D Fund from the Ministry of Science and Technology.

References

1. Hart, R.D., 1981, A fully coupled thermal-mechanical fluid flow model for nonlinear geologic system, PhD. Thesis, Univ. of Minn., Minnesota
2. Hokmark, H., 1990, Distinct element method of fracture behavior in near field rock, Stripa Project 91-01, SKB
3. Hokmark, H. and Israelsson, I., 1991, Distinct

element modeling of joint behavior in nearfield rock, Stripa Project 91-22, SKB
4. Itasca Consulting Group, Inc., 1996, DEC(Universal Distinct Element Code), version 3.0, Minneapolis, Minnesota
5. Johansson, E., Hakala, M. and Lorig, L.J. 1991, Rock mechanical, thermomechanical, and hydraulic behavior of the near field for spent nuclear fuel, Report YJT-91-21, TVO, Helsinki
6. Kang, C.H. et al., 2000, Preliminary conceptual design and performance assessment of a deep geological repository for high level wastes in the Republic of Korea, KAERI and Sandia National Lab., Rep. of Korea
7. Noorishad, J., Tsang, C.F. and Witherspoon, P.A. 1984, Coupled thermal- hydraulic-mechanical phenomenon in saturated fractured porous rocks-numerical approach, Jour. Geophy. Res., 89
8. Shen, B. and Stephansson, O., 1990, Rock mass response to glaciation and thermal loading from nuclear waste, Proc. GEOVAL-90 Symp., Stockholm
9. SKB, 1997, Results from pre-investigations and detailed site characterizations: Summary Report, Aspo HRL-Geoscientific Evaluation 1997/2. SKB Technical Report 97-03
10. SKB, 1997, Results from pre-investigations and detailed site characterization: Summary Report, Aspo HRL-Geoscientific Evaluation 1997/2, SKB Technical Report 97-04
11. Tsang, C.F., 1990, Coupling behavior of rock joints, in Rock Joints(edited by N. Barton and O. Stephansson)

투 고 일 2003년 3월 3일
심 사 일 2003년 3월 4일
심사완료일 2003년 4월 16일

김진웅
한국원자력연구소 방사성폐기물처분연구부
305-353 대전광역시 유성구 덕진동 150
Tel: 042-868-2018
E-mail : njwkim@kaeri.re.kr

배대석
한국원자력연구소 방사성폐기물처분연구부
305-353 대전광역시 유성구 덕진동 150
Tel: 042-868-2030
E-mail : ndsbae@kaeri.re.kr